Inorg. Chem. **2004**, *43*, 4447−4455

Stabilization of Calcium− and Terbium−Carboxylate Bonds by NH···O Hydrogen Bonds in a Mononuclear Complex: A Functional Model of the Active Site of Calcium-Binding Proteins

Akira Onoda,[†] Yusuke Yamada,[†] Yoshiki Nakayama,[†] Kazuyuki Takahashi,[†] Hiroshi Adachi,[†] Taka-aki Okamura,[†] Akira Nakamura,[‡] Hitoshi Yamamoto,[†] Norikazu Ueyama,*[,†] Drahomir Vyprachticky,[§,||] and Yoshi Okamoto*[,§]

Department of Macromolecular Science, Graduate School of Science, Osaka University, Toyonaka, Osaka 560-0043, Japan, and OM Research, 7-2-1308, Minami Ogimachi, Osaka 530-0025, Japan, and Polymer Research Institute and Department of Chemistry, Polytechnic University, 6-Metrotech Center, Brooklyn, New York 11201

Received September 10, 2003

Novel benzoic acid ligands with bulky amide groups at the *ortho* position, 2,6-$(MeCONH)_2C_6H_3CO_2H$ (**1**) and 2,6-$(t\text{-}BuCONH)_2C_6H_3CO_2H$ (**2**), and their tris- and tetrakis(carboxylate) complexes with Ca(II) and Tb(III) ions, $(NEt_4)_2[Ca^{II}\{O_2C\text{-}2,6\text{-}(t\text{-}BuCONH)_2C_6H_3\}_4]$ (**4**), $[Tb\{O_2C\text{-}2,6\text{-}(t\text{-}BuNHCO)_2C_6H_3\}_3(H_2O)_3\}]$ (**5**), and $(NMe)_4[Tb\{O_2C\text{-}2,6\text{-}(t\text{-}BuNHCO)_2C_6H_3\}_4(thf)]$ (**6**), were synthesized. The formation of the NH···O hydrogen bonds between the amide NH and carboxylate for **2**, $(NEt_4)\{2,6\text{-}(t\text{-}BuCONH)_2C_6H_3CO_2\}$ (**3**), and **4** was determined by ^1H NMR spectroscopy in solution and in the solid state (CRAMPS, IR). The ligand exchange reactions were attempted between **4** and a large excess of 2,4,6- $Me_3C_6H_3CO_2H$ in chloroform-*d* solution; however, exchange reaction did not take place, indicating that the Ca(II) ions bound strongly to the carboxylate in **4**. The Ca(II) ion binding properties with the benzoate derivatives were also examined using Tb(III) ion as a fluorescence probe. These results indicate that the NH···O hydrogen bonding between the amide NH and the oxygen atom of the carboxylate contributes to strong Ca(II) binding and prevents the dissociation of the calcium−carboxylate bond. The X-ray structural analyses of these complexes revealed that the NH···O hydrogen-bonded carboxylate ligands prefer the chelate-type coordination and create a mononuclear $\{Ca(O_2CR)_4\}^{2-}$ or $\{Tb(O_2CR)_4\}^-$ core with anionic charge, which is known only in the active site of calcium-binding proteins.

Introduction

Most calcium-mediated biochemical processes result from the direct binding of the Ca(II) ion to specific and selective sites on the calcium-binding proteins,[1] such as troponin C,[2−4] calmodulin,[5,6] and parvalbumin.[7−9] Crystal structure analyses of these proteins reveal that the binding site has a characteristic structural EF-hand motif consisting of a helix−loop−helix region.[10] A member of the EF-hand family of calcium-binding proteins often relays a signal via a conformational change to the rest of the ligating proteins, and such a process of conformational change is still of recent interest.[4,11−15] Ca(II)-binding sites often lie within loops and side chain groups

* Authors to whom correspondence should be addressed. E-mail: ueyama@chem.sci.osaka-u.ac.jp (N.U.)
[†] Osaka University.
[‡] OM Research.
[§] Polytechnic University.
[||] On leave from the Institute of Macromolecular Chemistry, Academy of Science of the Czech Republic, 162-06 Prague, Czech Republic.

(1) Strynadka, N. C. J.; James, M. N. G. In *Encyclopedia of Inorganic Chemistry*; King, R. B., Ed.; John Wiley and Sons: Chichester, U.K., 1994; Vol. 1, pp 477−507.
(2) Sia, S. K.; Li, M. X.; Spyracopoulos, L.; Gagne, S. M.; Liu, W.; Putkey, J. A.; Sykes, B. D. *J. Biol. Chem.* **1997**, *272*, 18216−18221.
(3) Herzberg, O.; James, M. N. G. *J. Mol. Biol.* **1988**, *203*, 761−779.
(4) Wang, X.; Li, M. X.; Spyracopoulos, L.; Beier, N.; Chandra, M.; Solora, R. J.; Sykes, B. D. *J. Biol. Chem.* **2001**, *276*, 25456−25466.
(5) Babu, Y. S.; Bugg, C. E.; Cook, W. J. *J. Mol. Biol.* **1988**, *204*, 191−204.
(6) Wilson, M. A.; Brunger, A. T. *J. Mol. Biol.* **2000**, *301*, 1234−1256.
(7) Swain, A. L.; Kretsinger, R. H.; Amma, E. L. *J. Biol. Chem.* **1989**, *220*, 1017.
(8) Declercq, J. P.; Tinant, B.; Parello, J.; Rambaud, J. *J. Mol. Biol.* **1991**, *220*, 1017−1039.
(9) Declercq, J. P.; Evrard, C.; Lamzin, V.; Parello, J. *Protein Sci.* **1999**, *8*, 2194−2024.
(10) Krestsinger, R. H.; Barry, C. D. *Biochim. Biophys. Acta* **1975**, *405*, 40−52.

10.1021/ic035075t CCC: $27.50
Published on Web 06/11/2004

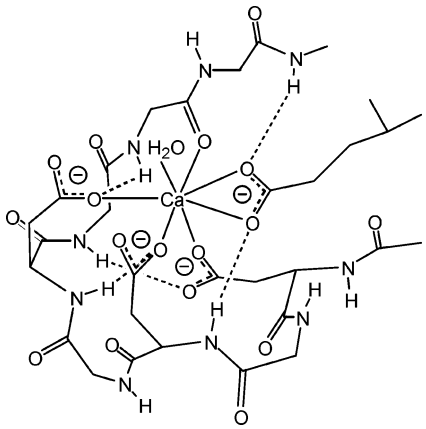

Figure 1. Calcium-binding site with four carboxylate goups in parvalbumin. Coordinating carboxylates are NH···O hydrogen-bonded with main chain NH groups within the Asx turn.

of aspartates, glutamates, glutamines, the main chain amide carbonyl, and water molecules. The mononuclear Ca(II) ion coordinated with three or four carboxylates has been known to give an anionic Ca(II) core, which has not been synthetically obtained. In addition, most of the coordinating carboxylate groups are involved in an Asx turn, where the side chain at position *n* is hydrogen-bonded with the main chain NH of a residue at position $n + 2$,[3,16] as shown in Figure 1.[17] The NH···O hydrogen bonds in the active site of the calcium-binding proteins have been hitherto proposed to contribute to their structural stabilization.[1] In the calcium-binding proteins, a remarkable increase in the metal ion binding has been observed.[1] This is an important basic condition for Ca-binding in many of these proteins.

We focus on the roles of the conserved NH···O hydrogen bonds to carboxylate groups in the active site and the relationship with their binding properties. We have investigated the functions of the NH···X hydrogen bonds to the coordinated atom as a model of the active site of the metalloproteins. Our previous studies on NH···S hydrogen bonds in iron−sulfur proteins and in P-450 model complexes have demonstrated that the intramolecular NH···S hydrogen bonds shift positively the redox potential of iron and protect the Fe−S bond from dissociation because of the stabilization of the anionic thiolate state by the NH···S hydrogen bonds.[18−22] Such a stabilization of the ligand anion is also expected by NH···O hydrogen bonds in carboxylate coordination. We have shown previously that some dicarboxylate or poly(carboxylate) ligands connected with an amide group bind strongly to the calcium ions.[23−25] Thus, we are motivated to clarify the effect of NH···O hydrogen bonds in coordinating carboxylate ligands for the Ca(II) ion binding using simplified hydrogen-bonded analogues.

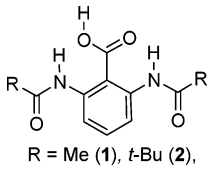

R = Me (**1**), *t*-Bu (**2**),

Figure 2. Intramolecularly NH···O hydrogen-bonded benzoate ligands.

We have prepared the benzoate ligands with bulky amide substituents on the *ortho* positions, 2,6-$(MeCONH)_2C_6H_3CO_2H$ (**1**) and 2,6-$(t\text{-}BuCONH)_2C_6H_3CO_2H$ (**2**), as shown in Figure 2. These ligands are expected to have stable intramolecular six-membered NH···O hydrogen bonds and also to prevent the formation of the polymeric complexation with steric congestion. First, we investigated the formation of intramolecular NH···O hydrogen bonds in various benzoate complexes in a chloroform solution by ^{1}H NMR measurements. Second, we studied in detail the effect of the NH···O hydrogen bonds on the Ca(II) ion binding with the carboxylate in a solution using Tb(III) ions as fluorescence probes. Finally, we prepared single crystals of the series of the Ca(II) and Tb(III)−benzoate complexes $(NEt_4)_2[Ca\{O_2C\text{-}2,6\text{-}(t\text{-}BuCONH)_2C_6H_4\}_4]$ (**4**), $[Tb\{O_2C\text{-}2,6\text{-}(t\text{-}BuNHCO)_2C_6H_3\}_3(H_2O)_3\}]$ (**5**), and $(NMe)_4[Tb\{O_2C\text{-}2,6\text{-}(t\text{-}BuNHCO)_2C_6H_3\}_4(thf)]$ (**6**). The formations of the intramolecular NH···O hydrogen bonds in the solid state are analyzed by crystal structures and IR and ^{1}H NMR CRAMPS (combined rotation and multipulse spectroscopy) measurements. On the basis of these results, we will present a chemical role of the NH···O hydrogen bonds to the carboxylate group and the effect on the calcium−oxygen bonds.

Experimental Section

Materials. All solvents were distilled over appropriate drying agents and degassed prior to use. All starting reagents were of commercial grade. Syntheses of 2,6-$(MeCONH)_2C_6H_3CO_2H$ (**1**), 2,6-$(t\text{-}BuCONH)_2C_6H_3CO_2H$ (**2**), $(NEt_4)\{2,6\text{-}(t\text{-}BuCONH)_2C_6H_3CO_2\}$ (**3**), 2-*t*-$BuCONHC_6H_4SO_3Na$, and 4-*t*-$BuCONHC_6H_4SO_3Na$ were reported previously.[26−28]

(11) Li, M. X.; Spyracopoulos, L.; Sykes, B. D. *Biochemistry* **1999**, *38*, 8289−8298.
(12) Li, Y.; Love, M. L.; Putkey, J. A.; Cohen, C. *Proc. Natl. Acad. Sci. U.S.A.* **2000**, *97*, 5140−5145.
(13) Elshorst, B.; Hennig, M.; Forsterling, H.; Diener, A.; Maurer, M.; Schulte, P.; Schwalbe, H.; Griesinger, C.; Krebs, J.; Schmid, H.; Vorherr, T.; Carafoli, E. *Biochemistry* **1999**, *38*, 12320−12332.
(14) Mirzoeva, S.; Weigand, S.; Lukas, T. J.; Shuvalova, L.; Anderson, W. F.; Watterson, D. M. *Biochemistry* **1999**, *38*, 3936−3947.
(15) Chou, J. J.; Li, S.; Kee, C. B.; Bax, A. *Nat. Struct. Biol.* **2001**, *8*, 990−997.
(16) Baker, E. N.; Hubbard, R. E. *Prog. Biophys. Mol. Biol.* **1984**, *44*, 97−179.
(17) Declerq, J. P.; Tinant, B.; Parello, J.; Etienne, G.; Huber, R. *J. Mol. Biol.* **1988**, *202*, 349−353.
(18) Ueyama, N.; Yamada, Y.; Okamura, T.; Kimura, S.; Nakmura, A. *Inorg. Chem.* **1996**, *35*, 6473−6484.
(19) Ueyama, N.; Nishikawa, N.; Yamada, Y.; Okamura, T.; Nakamura, A. *J. Am. Chem. Soc.* **1996**, *118*, 12826−12827.
(20) Ueyama, N.; Inohara, M.; Onoda, A.; Ueno, T.; Okamura, T.; Nakamura, A. *Inorg. Chem.* **1999**, *38*, 4028−4031.
(21) Ueno, T.; Kousumi, Y.; Yoshizawa-Kumagaye, K.; Nakajima, K.; Ueyama, N.; Okamura, T.; Nakamura, A. *J. Am. Chem. Soc.* **1998**, *120*, 12264−12273.
(22) Ueno, T.; Nichikawa, N.; Moriyama, S.; Adachi, S.; Lee, K.; Okamura, T.; Ueyama, N.; Nakamura, A. *Inorg. Chem.* **1999**, *38*, 1199−1210.
(23) Ueyama, N.; Hosoi, T.; Yamada, Y.; Doi, M.; Okamura, T.; Nakamura, A. *Macromolecules* **1998**, *31*, 7119−7126.
(24) Ueyama, N.; Takeda, J.; Yamada, Y.; Onoda, A.; Okamura, T.; Nakamura, A. *Inorg. Chem.* **1999**, *38*, 475−478.
(25) Ueyama, N.; Kozuki, K.; Doi, M.; Yamada, Y.; Takahashi, K.; Onoda., A.; Okamura, T.; Yamamoto, H. *Macromolecules* **2001**, *34*, 2607−2614.
(26) Yamada, Y.; Ueyama, N.; Okamura, T.; Mori, W.; Nakamura, A. *Inorg. Chim. Acta* **1998**, *275*−*276*, 43−51.
(27) Onoda, A.; Yamada, Y.; Takeda, J.; Nakayama, Y.; Okamura, T.; Doi, M.; Yamamoto, H.; Ueyama, N. *Bull. Chem. Soc. Jpn.* **2004**, *77*, 321−329.

$(NEt_4)_2[Ca\{O_2C\text{-}2,6\text{-}(t\text{-}BuCONH)_2C_6H_4\}_4]$ (4). To 5 mL of an aqueous solution of $Ca(OAc)_2 \cdot H_2O$ (5.45 mg, 3.09×10^{-2} mmol) and $(NEt_4)(OAc) \cdot 4H_2O$ (16.3 mg, 6.24×10^{-2} mmol) was added an EtOH (10 mL) solution of 2,6-(*t*-BuCONH)$_2$C$_6$H$_4$CO$_2$H (50 mg, 1.56×10^{-1} mmol). The mixed solution was evaporated, and the residue was recrystallized from CH_3CN/diethyl ether to give colorless prismatic crystals. Yield: 35 mg (72%). Anal. Calcd for $C_{84}H_{132}N_{10}O_{16}Ca$: C, 63.93; H, 8.43; N, 8.88. Found: C, 64.03; H, 8.51; N, 8.51. ESI-MS [calcd (found) *m*/*e*]: $(NEt_4)[Ca\{O_2C\text{-}2,6\text{-}(t\text{-}BuCONH)_2C_6H_4\}_4]^-$, 1446.8 (1445.8).

$[Tb\{O_2C\text{-}2,6\text{-}(t\text{-}BuNHCO)_2C_6H_3\}_3(H_2O)_3\}]$ (5). To $Tb(OAc)_3$ (31 mg, 9.2×10^{-5} mol) in 9.1 mL of ethanol solution was added 2,6-(*t*-BuCONH)$_2$C$_6$H$_3$CO$_2$H (88 mg, 2.8×10^{-4} mol) in 5.5 mL of acetonitrile. After evaporation of all solvents under reduced pressure, the obtained residue was recrystallized from THF/diethyl ether. Colorless prismatic crystals were obtained. Yield: 21 mg (18%). Anal. Calcd for $C_{51}H_{69}N_6O_{12}Tb \cdot H_2O$: C, 53.97; H, 6.30; N, 7.40. Found: C, 54.26; H, 6.74; N, 7.41. ESI-MS [calcd (found) *m*/*e*]: $[Tb\{O_2C\text{-}2,6\text{-}(t\text{-}BuCONH)_2C_6H_4\}_3] + Na^+$, 1139.4 (1140.7).

$(NMe_4)[Tb\{O_2C\text{-}2,6\text{-}(t\text{-}BuNHCO)_2C_6H_3\}_4(thf)]$ (6). To 2,6-(*t*-BuCONH)$_2$C$_6$H$_3$CO$_2$H (163.4 mg, 5.10×10^{-4} mol) in 20 mL of MeCN was added an EtOH solution (8.0 mL) of $(NMe_4)(OAc)$ (16.9 mg, 1.27×10^{-4} mol) and $Tb(OAc)_3$ (56.4 mg, 1.27×10^{-4} mol). The solution was refluxed for 12 h. After evaporation of all solvents under reduced pressure, the obtained residue was recrystallized from THF/diethyl ether. Colorless prismatic crystals were obtained. Yield: 69 mg (31%). Anal. Calcd for $C_{72}H_{104}N_9O_{16}Tb \cdot (THF)_{1.5} \cdot (H_2O)_3$: C, 56.00; H, 7.35; N, 7.54. Found: C, 55.98; H, 7.33; N, 7.45. ESI-MS [calcd (found) *m*/*e*]: $[Tb\{O_2C\text{-}2,6\text{-}(t\text{-}BuCONH)_2C_6H_4\}_4]^-$, 1435.6 (1435.7).

4-*t*-BuCONHC$_6$H$_4$COOH. To 4-aminobenzoic acid (5.0 g, 36 mmol) in 100 mL of THF solution was slowly added pivaloyl chloride (4.4 g, 36 mmol) at 0 °C. The solution was stirred for 1 h, and the 4% $NaHCO_3$(aq) solution (100 mL) was added. THF was removed under reduced pressure. After acidification to pH 1 by 10% HCl(aq) solution, the product was extracted with ethyl acetate. The organic layer was dried over Na_2SO_4, and the solvent was removed under reduced pressure. The residue was recrystallized from hot MeOH. Yield: 3.0 g (38%). Anal. Calcd for $C_{12}H_{15}NO_3$: C, 65.14; H, 6.85; N, 6.33. Found: C, 64.91; H, 6.84; N, 6.39. ^{1}H NMR (DMSO-d_6): δ 12.6 (s, 1H), 9.43 (s, 1H), 7.87 (d, 2H), 7.88 (d, 2H), 1.25 (s, 9H).

Physical Measurements. ^{1}H NMR spectra were taken on JEOL EX-270 and GSX-400 spectrometers using $CDCl_3$ solution. Mass spectrometric analyses were performed on a solution using a FinniganMAT LCQ mass spectrometer and a JEOL LCMATE mass spectrometer equipped with an ESI interface. Excitation and emission spectra were measured by a Perkin-Elmer LS-50B luminescence spectrophotometer. pK_a and K measurements were performed in 10 mM carboxylic acid compounds with 1 equiv of Ca ion in aqueous solution at 25 °C using potentiometric titration. The saturated calomel glass electrode purchased from Metrohm was calibrated with a 0.05 M $KHC_8H_4O_4$ buffer (pH 4.01) and a 0.025 M KH_2PO_4/0.025 M Na_2HPO_4 buffer (pH 6.86). ^{1}H NMR CRAMPS (combined rotation and multipulse spectroscopy) was recorded on a Chemmagnetics CMX-300 and measured with a 4 mm φ pencil rotor cell using a BR-24 multiple-pulse sequence.[29] IR spectra were recorded on a Jasco FT-IR 8300 spectrometer. Samples were prepared as KBr pellets.

Table 1. Crystallographic Data for **4**−**6**

	4·$(CH_3CN)(Et_2O)$	**5**·$(H_2O)_2(THF)$	**6**·$(THF)_{3.5}$
empirical formula	$C_{92}H_{148}CaN_{12}O_{17}$	$C_{55}H_{87}N_6O_{18}Tb$	$C_{90}H_{140}N_9O_{20.5}Tb$
fw	1734.30	1279.23	1835.03
color	colorless	colorless	colorless
cryst syst	monoclinic	monoclinic	monoclinic
lattice params			
a, Å	24.67(4)	18.464(2)	14.1181(4)
b, Å	18.26(3)	13.6955(14)	25.0087(7)
c, Å	22.58(3)	26.228(4)	27.8505(7)
α, deg	90	90	90
β, deg	104.58(5)	109.301(4)	100.188(1)
γ, deg	90	90	90
V, Å^3	9843(26)	6259.7(14)	9678.3(5)
space group	*Cc* (No. 9)	$P2_1/n$ (No. 14)	$P2_1/n$ (No. 14)
Z	4	4	4
ρ_{calcd}, g cm^{-1}	1.170	1.357	1.259
μ(Mo Kα), cm^{-1}	1.310	1.201	0.800
temp (K)	100	200	200
scan type	ω	ω	ω
no. of collected reflns	48188	50382	77771
no. of unique reflns	20556	13038	21784
no. of obsd data ($I > 2\sigma(I)$)	7744	7867	10274
no. of variables	1091	749	1029
GOF	1.000	0.0989	1.000
R1[a]	0.056	0.064	0.063
wR2[b]	0.083	0.158	0.111

[a] $R1 = \sum||F_o| - |F_c||/\sum|F_o|$ [$I > 2\sigma(I)$]. [b] $wR2 = [\sum w(F_o^2 - F_c^2)^2/\sum w(F_o^2)^2]^{1/2}$.

X-ray Structure Determination. The X-ray data for **4** were collected in 2.0° oscillations at 100 K on a Raxis RAPID instrument. **5** and **6** were collected in 2.0° oscillations at 200 K. Sweeps of data for **4** were done using ω oscillations from 130.0° to 190.0° at $\phi = 50.0°$ and $\chi = 45.0°$ and from 0.0° to 160.0° at $\phi = 230.0°$ and $\chi = 45.0°$, for **5** from 130.0° to 190.0° at $\phi = 0.0°$ and $\chi = 45.0°$, and for **6** from 0.0° to 160.0° at $\phi = 180.0$ ° and $\chi = 45.0°$. The basic crystallographic parameters for **4**−**6** are listed in Table 1. The structures were solved by the direct method and expanded using Fourier techniques using teXsan crystallographic software[30] and SHELXL-97.[31] The following non-hydrogen atoms were refined using isotropic displacement parameters: disordered methyl carbon atoms in two *t*-Bu groups, atoms in a disordered ether molecule, and atoms in a MeCN solvent molecule in **4**; disordered methyl carbon atoms in one *t*-Bu group in **5**; disordered methyl carbon atoms in two *t*-Bu groups, atoms in solvent THF molecules, and carbon atoms in a coordinating THF molecule in **6**. Other non-hydrogen atoms were refined with anisotropic displacement parameters. Hydrogen atoms except for those riding on H_2O oxygen atoms for **5** and those of the solvent molecules for **6** were placed in idealized positions and refined isotropically to be constrained to ride on their parent atom. The following restraints were used: for **4**, the distances in the disordered diethyl ether were restrained by SADI or DFIX, the bond lengths in the disordered MeCN were restrained by SADI, and the thermal parameters of disordered atoms in the ether were fixed to the corresponding atom by EADP; for **5**, the disordered *t*-Bu groups were restrained by SADI ($C-CH_3$, CH_3---CH_3) and SIMU and DELU (CH_3); for **6**, the weak reflections gave the THF molecules an unreasonable structure during the refinement, the molecules were restrained using DFIX and SADI, and the thermal parameters in each THF molecule were restrained by SIMU.

(28) Onoda, A.; Yamada, Y.; Doi, M.; Okamura, T.; Ueyama, N. *Inorg. Chem.* **2001**, *40*, 516−521.
(29) Burum, D. P.; Rhim, W. K. *J. Chem. Phys.* **1979**, *71*, 944−956.
(30) *teXsan: Crystal Structure Analysis Package*; Molecular Structure Corp., 1985, 1999.
(31) Sheldrick, G. M. *SHELXL-97, Program for the Refinement of Crystal Structure*; Univeristy of Gottingen: Gottingen, Germany, 1997.

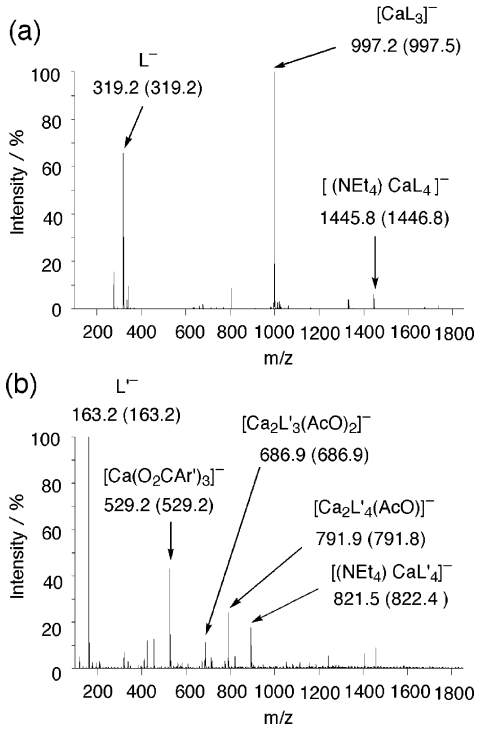

Figure 3. ESI-MS spectra of the mixed solution of (a) $(NEt_4)[Ca(OAc)_4]$ and 4 equiv of 2,6-(*t*-$BuCONH)_2C_6H_3CO_2H$ (**2**) and (b) $(NEt_4)[Ca(OAc)_4]$ and 4 equiv of 2,4,6-$Me_3C_6H_2CO_2H$ (negative mode).

Scheme 1

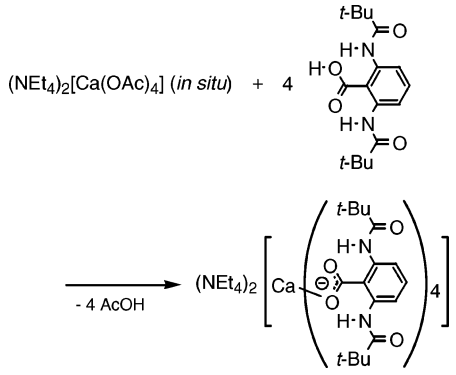

Results and Discussion

Synthesis of the Ca(II) Complex. Synthesis of the Ca(II) complex with the bulky amidated benzoate ligand was examined by the ligand exchange reaction in MeOH/water as shown in Scheme 1. The formation of the Ca−carboxylate complex was detected by ESI-MS. The measurement was performed with a mixed solution of $Ca(OAc)_2$ (5 mM), 2 equiv of Et_4NOAc (10 mM), and 4 equiv of 2,6-(*t*-$BuCONH)_2C_6H_3CO_2H$ (=$ArCO_2H$) in MeOH/water (4:1, v/v) in negative ion mode. We found fragments originating from the mononuclear Ca(II) complex, $[Ca(O_2CAr)_3]^-$ and $(NEt_4)[Ca(O_2CAr)_4]^-$ (Figure 3a). The observed species does not change with increasing ratio of $[ArCO^{2-}]$ to $[Ca^{2+}]$ up to 6 equiv. Thus, only the mononuclear tetrakis(carboxylato) complex is present, while, in a similar ESI-MS experiment using a mixture with non-hydrogen-bonded *ortho*-substituted benzoic acid, 2,4,6-$Me_3C_6H_2CO_2H$ ($Ar'CO_2H$), we observe fragments assigned to both mononuclear and binuclear Ca(II) complexes (Figure 3b). The benzoate ligand with bulky amide groups on the *ortho* position preferentially forms a mononuclear Ca(II) core.

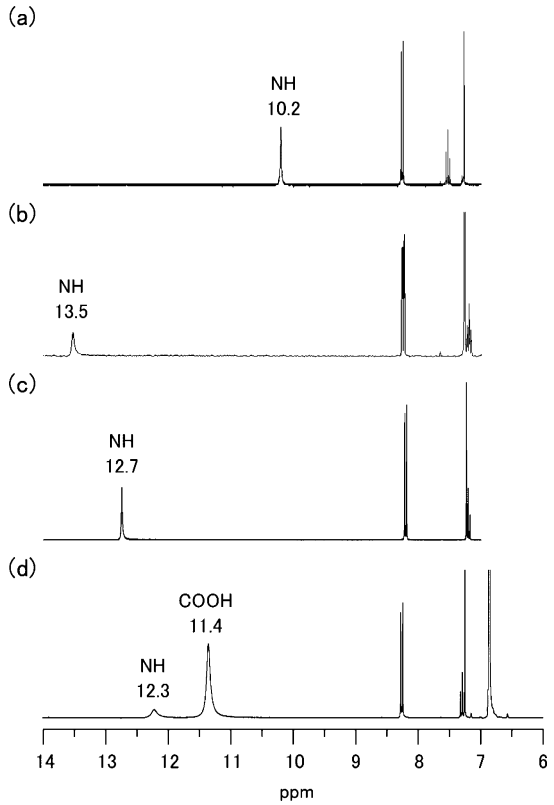

Figure 4. ^1H NMR spectra of (a) 2,6-(*t*-$BuCONH)_2C_6H_3CO_2H$ (**2**), (b) (NEt_4){2,6-(*t*-$BuCONH)_2C_6H_3CO_2$}, (c) $(NEt_4)_2[Ca\{O_2C$-2,6-(*t*-$BuCONH)_2C_6H_3\}_4]$ (**2**), and (d) $(NEt_4)_2[Ca\{O_2C$-2,6-(*t*-$BuCONH)_2C_6H_3\}_4]$ + 40 equiv of 2,4,6-$Me_3C_6H_2CO_2H$ in $CDCl_3$ (5 mM).

^1H NMR Spectroscopy in Solution. The formation of the NH···O hydrogen bonds in the solution state was determined by the ^1H NMR measurement in a 10 mM $CDCl_3$ solution (Figure 4). The amide NH chemical shift for **2**−**4** appears at 10.2, 13.5 and 12.7 ppm, respectively. In the carboxylic acid state, the amide ν(NH) stretching band for **2** is present at 3444 cm^{-1}, indicating that NH···O hydrogen bonds are not formed. The NH signal for carboxylate anion **3** shifts largely downfield (+3.3 ppm), while that for Ca(II) complex **4** shows less shift (+2.5 ppm). The results indicate that, in the formation of the NH···O hydrogen bond in these ligands, however, the hydrogen bonding in the Ca(II) complex is a little weaker than that in the carboxylate anion.

Ligand Exchange Reaction Detected by ^1H NMR Spectroscopy. To evaluate the effect of the NH···O hydrogen bonds on the calcium−carboxylate bond, we examined the ligand exchange reaction between the NH···O hydrogen-bonded calcium complex. The reaction was determined by ^1H NMR utilizing the amide NH chemical shift as a probe. The NH chemical shifts provide information for the electronic state of a carboxyl group, COOH, COO^-, and COO−Ca. We have performed the ligand exchange reaction between the NH···O hydrogen-bonded calcium complex, **4**, and 40 equiv of the non-hydrogen-bonded benzoate ligand 2,4,6-trimethylbenzoic acid. The results are shown in Figure 4d. In the absence of 2,4,6-trimethylbenzoic acid, the amide

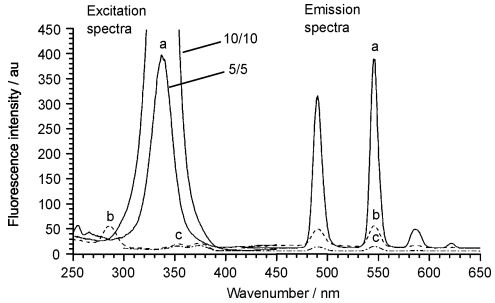

Figure 5. Luminescence excitation (em = 545 nm) and emission (excited at maximum spectra for Tb^{3+}−ligand (1:1) complexes in water ($[Tb^{3+}]$ = [ligand] = 5 mM). Ligands are (a) 2,6-$(MeCONH)_2C_6H_3CO_2H$ (**1**) and (b) $C_6H_5CO_2H$. (c) is for the comcpound without ligands. The spectra were taken in phosphorescence mode with a 0.05 ms delay.

NH chemical shift for **4** appears at 12.7 ppm. When the amide-containing ligand dissociates as a carboxylic acid state, we can observe the upfield-shifted NH around 10.2 ppm, while, with the addition of the excess 2,4,6-trimethylbenzoic acid, the NH signal still appears at 12.3 ppm. Thus, the amide ligands are in the carboxylate anion and coordinate to the Ca(II) ion. The ligand exchange reaction reveals that the calcium−carboxylate bond with the NH···O hydrogen-bonded ligand is prevented from dissociation more strongly than that with the NH···O non-hydrogen-bonded ligand.

Tb(III) Fluorescence Measurements in Aqueous Solution. The application of lanthanide ions such as Eu and Tb as a luminescence probe for Ca-binding proteins is well documented.[32,33] The metal ions that are native to metalloenzymes, for example, Ca, Mg, and Zn ions, are spectroscopically inactive. The substitution of trivalent lanthanides for those ions has been utilized in the elucidation of metal binding properties. The excitation and emission spectra of Tb(III) complexes with 2,6-$(MeCONH)_2C_6H_3CO_2H$ (**1**), 4-$NCC_6H_4CO_2H$, $C_6H_5CO_2H$, and Tb(III) ion without ligand are shown in Figure 5. The highest emission peak at 545 nm corresponds to the $^5D_4 \rightarrow {}^7F_6$ transition of the Tb(III) ion. In the absence of the ligands, the Tb(III) ion exists as an aquo complex, $[Tb(OH_2)_n]^{3+}$, with nine water molecules ($n = 9$) bound to the inner coordination sphere.[34] These coordinated water molecules serve as efficient quenchers of the intrinsic Tb(III) luminescence, and consequently, the emissive intensity of an aqueous terbium solution is normally very weak (Figure 5c). The OH stretching mode of the coordinated H_2O is effective at quenching the terbium $^5D_4$ excited state via nonradiative energy transfer. Thus, once the ligating groups occupy a specific coordination site on the Tb(III) ion, the luminescence intensity of the Tb(III) ion can be increased.[35] As shown in Figure 5, the emission intensities in hydrogen-bonded ligands are greatly increased: 2,6-$(MeCONH)_2C_6H_3CO_2H$ (**1**) (400) > $C_6H_5CO_2H$ (50) > Tb(III) ion alone (15). The fluorescence intensities plotted against the ratio of **1** to the Tb(III) ion are shown in Figure 6. The intensities reach a limiting value at a ratio of 6 and remain constant up to a ratio of 10 without exhibiting any turbidity in the solution.

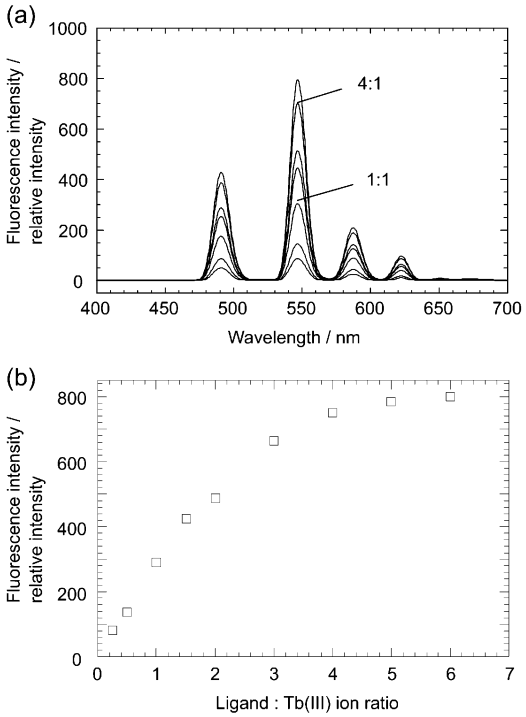

Figure 6. (a) Fluorescence spectra of Tb(III) ions with the addition of **1** ($[Tb^{3+}]$ = 5 mM) and (b)a plot of the fluorescence intensity at 545 nm and the ligand:Tb^{3+} ratio.

The increase of the fluorescence intensity upon the complex formation between the ligands and the Tb(III) ion may be due to two factors: (1) the discharge of the inner coordinated water molecules to Tb(III) upon the complex formation and (2) the energy transfer from the ligand to Tb(III). Horrocks and Sudnick have developed a quantitative method by which the number of coordinated water molecules to the Tb(III) ion can be determined on the basis of a deuterium isotope effect.[35] As mentioned above, water is a quencher of the intrinsic Tb(III) fluorescence through dissipation of the excitation energy by way of the OH manifold. Deuterated water has a greater reduced mass of the OD manifold. Hence, the number of coordinated water molecules is directly related to the difference in the emission lifetime as given in following equation: number of coordinated water molecules $= q\{\tau^{-1}{}_{H_2O} - \tau^{-1}{}_{D_2O}\}$ (2), where $q = 4.2$ ms^{-1} for Tb(III) and τ is the observed lifetime of the complex in H_2O or D_2O. Typical semilogarithmic plots of the experimental decay of the fluorescence intensity of the Tb(III) complexes with hydrogen-bonded benzoate (**1**) and benzoate are shown in Figure 7. The method of Horrocks was used to determine the number of water molecules bound to Tb(III), and the results are summarized in Table 2. The lifetime measurements correlate with the intensity data showing an average of 5.4 waters bound to Tb(III) in **1**. These results indicate that since nine water molecules are coordinated to the Tb(III) ion in aqueous solution, about four coordinated water molecules are replaced with **1**, while benzoate ligand replaced less (about one coordinated water molecule). Thus,

(32) Sowadski, J.; Cronick, G.; Kretsinger, R. H. *J. Mol. Biol.* **1978**, *124*, 123−132.
(33) Niebour, E. *Structure. Bonding* **1975**, *22*, 1.
(34) Chattergee, A.; Maslen, E. N.; Watson, K. J. *Acta Crystallogr.* **1988**, *B44*.
(35) Horrocks, W. D., Jr.; Sudnick, D. R. *Acc. Chem. Res.* **1981**, *14*, 384−392.

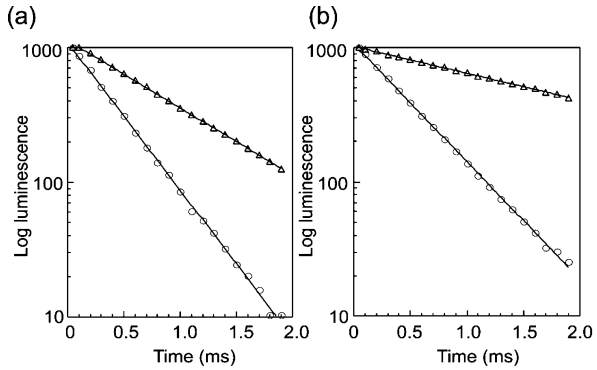

Figure 7. Lifetime measurement of Tb(III) fluorescence at 545 nm with the addition of 3 equiv of (a) 2,6-$(MeCONH)_2C_6H_3CO_2^-$ and (b) $C_6H_5CO_2^-$ (concentration of Tb(III) ion 5 mM, excited at (a) 344 nm (max) and (b) 295 nm (max)).

Table 2. Summary of Lifetime Measurements

ligand[a]	solvent	obsd rate constant (ms^{-1})	no. of coordinated water molecules[b]
2,6-$(MeCONH)_2C_6H_3CO_2^-$	D_2O	1.23	5.4
	H_2O	2.52	
$C_6H_5CO_2^-$	D_2O	0.45	6.6
	H_2O	2.02	
2-(*t*-BuCONH)$C_6H_4SO_3^-$	D_2O	3.84	9.8
	H_2O	1.50	
4-(*t*-BuCONH)$C_6H_4SO_3^-$	D_2O	0.68	9.1
	H_2O	2.85	
2-Me-$C_6H_4SO_3^-$	D_2O	0.48	8.6
	H_2O	2.53	

[a] The concentrations of the ligand and $TbCl_3 \cdot 6H_2O$ were 15 and 5 mM, respectively. λ_{ex} was at the maximum, and $\lambda_{em} = 545$ nm. [b] The constant of proportionality used was 4.2 ms^{-1}.

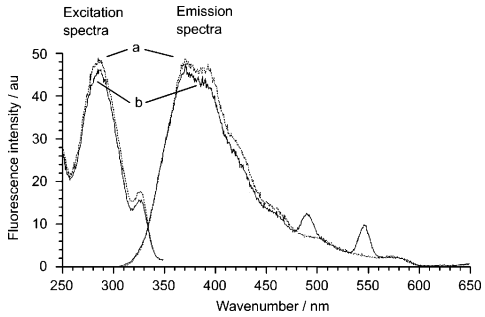

Figure 8. Fluorescence excitation (em = 370 nm) and emission (ex = 287 nm) spectra of (a) $C_6H_5CO_2H$ (**1**) in the absence and (b) in the presence of Tb(III). The spectra were taken in the fluorescence mode.

a hydrogen-bonded benzoate ligand binds stronger to Tb(III) than the benzoate and increases the Tb(III) fluorescence.

Energy transfer in the amide-containing benzoate ligand is also involved in the increasing fluorescence. **1** has a strong absorption at 340 nm, and the fluorescence emission is exhibited at 390 nm when **1** is excited at 340 nm as shown in Figure 8. With the addition of the Tb(III) ion (1:1 ratio of the ligand to Tb(III)) into the aqueous ligand solution, the fluorescence emission intensity of the ligand at 390 nm was decreased from 750 to 500, and simultaneously the characteristic emission of Tb(III) appeared at 490 and 545 nm (intensity ~100). In the case of benzoate ligand, the fluorescence emission at 370 nm was decreased only from 46 to 44, and the characteristic emission of Tb(III) at 545 nm appeared, but the intensity was only around 10 (Figure 9). These results suggest that the ligand to Tb(III) energy

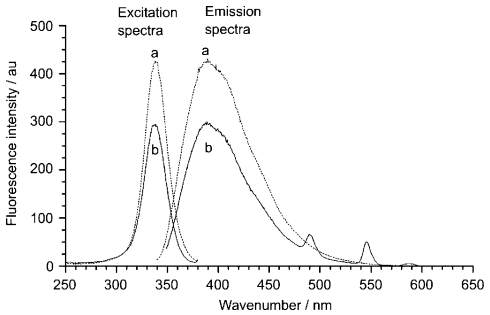

Figure 9. Fluorescence excitation (em = 390 nm) and emission (ex = 338 nm) spectra of (a) 2,6-$(MeCONH)_2C_6H_3CO_2H$ (**1**) in the absence and (b) in the presence of Tb(III). The spectra were taken in the fluorescence mode.

transfer in **1** is much larger than that of benzoate. The degree of energy transfer depends on the amount of overlap of the emission peak of the ligands (as an energy donor) on the absorption spectrum of Tb(III) ion. However, at present, we are not able to determine how much this energy transfer contributes to the increase in the fluorescence intensity for the Tb(III) and hydrogen-bonded benzoate complex.

To elucidate the effect of similar NH···O hydrogen bonds with the sulfonate ligands, such as 2-*t*-$BuCONHC_6H_4SO_3$-Na, 4-*t*-$BuCONHC_6H_4SO_3Na$, and 4-$MeC_6H_4SO_3Na$, we also measured the fluorescence lifetime of the Tb(III) ion with these sulfonate compounds. The numbers of coordinated water molecules calculated on Tb(III) with these sulfonates are cited in Table 2. These results indicate that the water molecules coordinated on Tb(III) are not expelled with these sulfonates and agree with our previous observation that the hydrogen bonding between the amide NH and sulfonate oxygen is weak due to the delocalization of the anion charge on the $-SO_3^-$ groups.[28] Thus, the hydrogen bonding between the amide NH and $-SO_3^-$ groups has little effect on the Ca(II) ion binding properties.

Measurements of Formation Constants of the Benzoic Acid Derivatives. We have measured the pK_a values of the benzoic acid compounds with the amide groups both in aqueous solution and in the aqueous micellar solution.[27] The pK_a value of water-insoluble carboxylic acid is obtainable in aqueous micellar solution due to the fast proton transfer.[36,37] The NH···O hydrogen bond works in hydrophobic environments, such as neutral micelles. Our previous results have indicated the NH···O hydrogen bond formation in **1** and **2** lowers the pK_a value of the carboxyl groups.[27]

The formation constants, *K*, with Ca(II) ion were determined using a potentiometric titration. We determined the *K* values of various carboxylic acid ligands for reference. The results are listed in Table 3. The *K* values clearly indicate that the formation constants increase when the pK_a values are lower. Thus, a lower shift of the pK_a value in NH···O hydrogen-bonded ligands contributes to the higher binding ability to the Ca ion.

The increased acidity of carboxylic acid by the NH···O hydrogen bonds can contribute to strong binding to a Ca(II)

(36) Cui, Q.; Karplus, M. *J. Am. Chem. Soc.* **2002**, *124*, 3093−3124.
(37) Pina, F.; Melo, M. J.; Alves, S.; Ballardini, R.; Maestri, M.; Passaniti, P. *New J. Chem.* **2001**, *25*, 747−752.

Table 3. Summary of pK_a and K Values of Carboxylic Acid Ligands

	log K^a	pK_a[a]		log K^a	pK_a[a]
2,6-(MeCONH)$_2$C$_6$H$_3$CO$_2$H	2.5	3.4	C$_6$F$_5$COOH	2.8	1.8
C$_6$H$_5$COOH	2.2	3.9	2,6-F$_2$C$_6$H$_3$CO$_2$H	3.8	2.1
CH$_3$COOH	2.2	4.5	3,5-F$_2$C$_6$H$_3$CO$_2$H	1.7	3.2

[a] K and pK_a values are measured at 25 °C (ionic strength 0.01).

ion. In general, the stability constant K between Ca(II) ion and carboxylate anion is defined by eq 1.

$$Ca^{2+} + ArCO_2^- \rightarrow Ca(ArCO_2)^+$$

$$K = [Ca(ArCO_2)^+]/[Ca^{2+}][ArCO_2^-] \quad (1)$$

However, when a Ca^{2+} ion reacts with the acid and forms the complex $Ca(ArCO_2)^+$, the complex formation constant, K_{HL}, can be defined as shown in eqs 2 and 3.

$$Ca^{2+} + ArCO_2H \rightarrow Ca(ArCO_2)^+ + H^+$$

$$K_{HL} = [Ca(ArCO_2)^+][H^+]/[Ca^{2+}][ArCO_2H]$$
$$= \{[Ca(ArCO_2)^+]/[Ca^{2+}][ArCO_2^-]\}\{[H^+][ArCO_2^-]/[ArCO_2H]\}$$
$$= KK_a \quad (2)$$

$$\log K_{HL} = \log K - pK_a \quad (3)$$

Thus, the complex formation constant, K_{HL}, can be dependent on both log K and pK_a values. The pK_a, log K, and calculated log K_{HL} values were reported for various carboxylate ligands.[38] The change of the pK_a values was found to be larger than that of the log K values of carboxylic acids, and the K_{HL} values are more sensitive to the pK_a values than the log K values. The benzoic acids having intramolecular hydrogen bonds with carboxylates, such as 2,6-di(hydroxyl)-benzoic acid and salicylic acid, have smaller pK_a values and larger log K_{HL} for binding with a Ca(II) ion.[39] Thus, we can also predict according to eq 3 that ligand **2** having lower a pK_a value forms stronger binding with a Ca(II) ion than those of the non-hydrogen-bonded benzoic acids.

X-ray Structures. The crystal structure of **4** is shown in Figure 10, and the selected bond distances and bond angles are listed in Table 4. Tetrakis(carboxylato) complex **4** has a mononuclear calcium core. Each ligand coordinates in a bidentate bridging (η^2) fashion. The Ca(II) center is eight-coordinate with dodecahedral geometry. There have been two examples of the mononuclear calcium core with a tetrakis-(carboxylato) chelating ligand. However, some of the carboxylate ligands in previous reports coordinate in μ_1 and μ_2 fashions to a neighboring Ca(II) ion.[40,41] Ca(II) complex **4** is the first homoleptic mononuclear one with −2 charge,

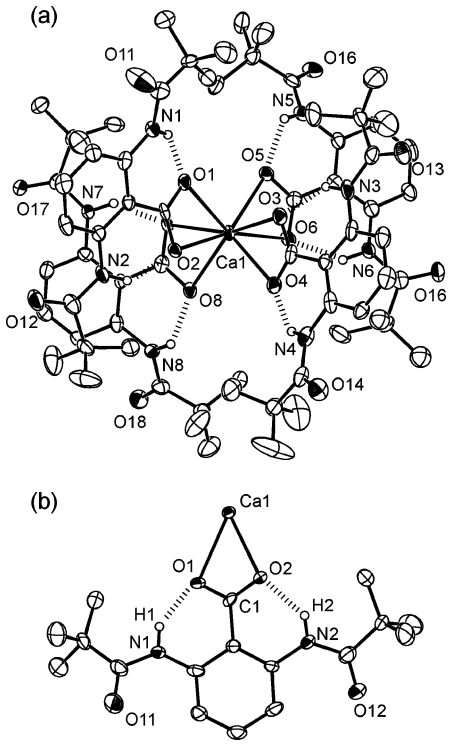

Figure 10. (a) Anion and (b) ligand structures of $(NEt_4)_2$[Ca{O_2C-2,6-(*t*-BuCONH)$_2$C$_6$H$_4$}$_4$] (**4**).

Table 4. Selected Bond Distances (Å) and Bond Angles (deg) for **4**

Bond Distances			
Ca(1)−O(1)	2.488(4)	Ca(1)−O(2)	2.434(4)
Ca(1)−O(3)	2.395(4)	Ca(1)−O(4)	2.542(4)
Ca(1)−O(5)	2.512(4)	Ca(1)−O(6)	2.443(4)
Ca(1)−O(7)	2.436(4)	Ca(1)−O(8)	2.484(4)
N(1)···O(1)	2.591(4)	N(2)···O(2)	2.583(5)
N(3)···O(3)	2.561(5)	N(4)···O(4)	2.586(5)
N(5)···O(5)	2.600(6)	N(6)···O(6)	2.600(4)
N(7)···O(7)	2.576(4)	N(8)···O(8)	2.590(5)
Bond Angles			
Ca(1)−O(1)−C(1)	91.9(3)	Ca(1)−O(2)−C(1)	94.1(3)
Ca(1)−O(3)−C(2)	97.1(2)	Ca(1)−O(4)−C(2)	89.9(3)
Ca(1)−O(5)−C(3)	90.7(3)	Ca(1)−O(6)−C(3)	94.3(3)
Ca(1)−O(7)−C(4)	93.2(3)	Ca(1)−O(8)−C(4)	90.6(2)

which can only be found in the Ca(II) center of calcium-binding proteins.

In the tetrakis complex, both amide NH groups are directed to the oxygen atoms of the carboxylate with short N···O distances. Usually the CO_2(carboxylate) plane and phenyl ring lie perpendicular each other when bulky groups are introduced in the *ortho* position.[42−48] The angle between the two planes is 17.2° (av) in **4**. Thus, the formation of double

(38) Martell, A. E.; Smith, R. M. *Critical Stability Constants*; Plenum Press: New York, 1974; Vol. 2.
(39) Eberson, L. In *The chemistry of carboxylic acids and esters*; Patai, S., Ed.; John Wiley and Sons: London, 1969; pp 211−293.
(40) Schauer, C. K.; Anderson, O. P. *J. Am. Chem. Soc.* **1987**, *109*, 3646−3456.
(41) Schauer, C. K.; Anderson, O. P. *J. Chem. Soc., Dalton Trans.* **1989**, 185−191.
(42) Lee, D.; Lippard, S. J. *J. Am. Chem. Soc.* **2001**, *123*.
(43) Lee, D.; Sorace, L.; Caneschi, A.; Lippard, S. J. *Inorg. Chem.* **2001**, *40*, 6774−6781.
(44) Lee, D.; Hung, P.-L.; Spingler, B.; Lippard, S. J. *Inorg. Chem.* **2002**, *41*, 521−531.
(45) Hagadorn, J. R.; Que, L., Jr.; Tolman, W. B. *J. Am. Chem. Soc.* **1998**, *120*, 1353113532.
(46) Hagadorn, J. R.; Que, L., Jr.; Tolman, W. B. *Inorg. Chem.* **2000**, *39*, 6086−6090.
(47) Anca, R.; Martinez-Carrera, S.; Garcia-Branco, S. *Acta Crystallogr.* **1967**, *23*, 1010.
(48) Kolotuchin, S. V.; Thiessen, P. A.; Fenlon, E. E.; Wilson, S. R.; Loweth, C. J.; Zimmerman, S. C. *Chemistry—Eur. J.* **1999**, *5*, 2537−2347.

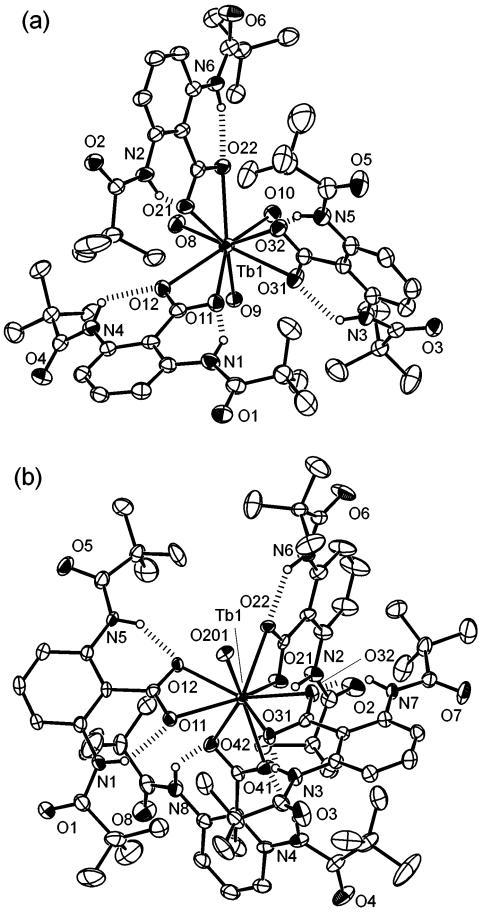

Figure 11. Molecular structure of (a) **[**Tb{O_2C-2,6-(*t*-BuNHCO)$_2$$C_6H_3$}$_3$·($H_2O$)$_3$}] (**5**) and (b) (NMe)$_4$[Tb{$O_2$C-2,6-(*t*-BuNHCO)$_2$$C_6H_3$}$_4$(thf)] (**6**). Carbon atoms of the THF molecule were omitted for clarity.

Table 5. Selected Bond Distances (Å) and Bond Angles (deg) for **5**

Bond Distances			
Tb(1)−O(8)	2.426(4)	Tb(1)−O(9)	2.379(4)
Tb(1)−O(10)	2.404(4)	Tb(1)−O(11)	2.432(4)
Tb(1)−O(12)	2.460(4)	Tb(1)−O(21)	2.378(4)
Tb(1)−O(22)	2.496(4)	Tb(1)−O(31)	2.495(4)
Tb(1)−O(32)	2.432(4)		
N(1)···O(11)	2.577(6)	N(2)···O(21)	2.543(6)
N(3)···O(32)	2.543(7)	N(4)···O(12)	2.584(7)
N(5)···O(22)	2.621(5)	N(6)···O(31)	2.588(7)
Bond Angles			
Tb(1)−O(11)−C(1)	96.0(4)	Tb(1)−O(12)−C(1)	94.6(4)
Tb(1)−O(21)−C(2)	96.8(3)	Tb(1)−O(22)−C(2)	92.6(3)
Tb(1)−O(31)−C(3)	93.0(4)	Tb(1)−O(32)−C(3)	95.7(4)

intraligand NH···O hydrogen bonds is thought to enforce the CO_2 plane to be almost coplanar with the phenyl plane.

Figure 11 shows the crystal structures of the Tb(III) complexes [Tb{O_2C-2,6-(*t*-BuNHCO)$_2$$C_6H_3$}$_2$($H_2O$)$_3$]] (**5**) and (NMe)$_4$[Tb{$O_2$C-2,6-(*t*-BuNHCO)$_2$$C_6H_3$}$_4$(thf)] (**6**). Selected bond distances and angles of **5** and **6** are listed in Tables 5 and 6, respectively. **5** has a mononuclear Tb(III) core coordinated with three carboxylate ligands in a bidentate chelate fashion (η^2) and three water oxygen atoms. The nine-coordination sphere gives a distorted tricapped trigonal prism. The two coordinated water oxygen atoms were OH···O═C hydrogen-bonded with amide carbonyl groups of neighboring units. **6** also has a mononuclear Tb(III) core with tetrakis-(carboxylate) coordination with a THF oxygen. The distances

Table 6. Selected Bond Distances (Å), Bond Angles (deg), and Torsion Angles (deg) for **6**

Bond Distances			
Tb(1)−O(11)	2.453(3)	Tb(1)−O(12)	2.384(3)
Tb(1)−O(21)	2.380(3)	Tb(1)−O(22)	2.488(3)
Tb(1)−O(31)	2.464(3)	Tb(1)−O(32)	2.395(3)
Tb(1)−O(41)	2.413(3)	Tb(1)−O(42)	2.479(3)
Tb(1)−O(201)	2.451(3)		
N(1)···O(11)	2.639(5)	N(2)···O(21)	2.547(5)
N(3)···O(31)	2.591(5)	N(4)···O(41)	2.569(5)
N(5)···O(12)	2.579(5)	N(6)···O(22)	2.605(5)
N(7)···O(32)	2.566(5)	N(8)···O(42)	2.573(5)
Bond Angles			
Tb(1)−O(11)−C(1)	91.9(3)	Tb(1)−O(12)−C(1)	96.0(3)
Tb(1)−O(21)−C(2)	97.2(3)	Tb(1)−O(22)−C(2)	92.0(3)
Tb(1)−O(31)−C(3)	92.2(3)	Tb(1)−O(32)−C(3)	96.0(3)
Tb(1)−O(41)−C(4)	97.0(3)	Tb(1)−O(42)−C(4)	93.8(3)

Chart 1. Three Typical Modes in Carboxylate−Metal Bindings

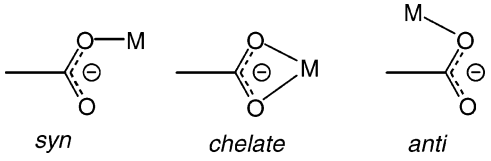

between amide N and carboxylate O atoms (2.543−2.639 Å) are within the hydrogen-bonding distance, and the amide NH protons exactly direct the carboxylate groups forward in both **5** and **6**.

The binding mode of the carboxylate groups in the complexation with metal ions can be classified by three types (Chart 1).[49−51] The first one is the *syn*-type coordination in which the M−O−C angle is nearly 120° in a clockwise direction. The second is the chelate type (η_2) in which the two oxygen atoms of the carboxylate coordinate to metal ions. The third is the *anti*-type coordination in which the M−O−C angle is nearly 240°. The *anti*-type coordination is frequently observed in polynuclear complexes, while our benzoate ligand with two strategically oriented bulky amide groups in the *ortho* position gives chelate-type coordination, which is basically important for a mononuclear structure as found in **4**−**6**. The NH···O hydrogen bonds to carboxylate groups presumably interact with the lone pair on the coordinating oxygen atoms and prohibit the *anti*-mode coordination.

Intramolecular Hydrogen Bonds in the Solid State. ^{1}H NMR spectroscopy (CRAMPS) is available to detect each proton under different circumstances in the solid state,[52] and we obtained spectra to confirm the formation of the NH···O hydrogen bonds. CRAMPS spectra of 2,6-(*t*-BuCONH)$_2$-$C_6H_3CO_2H$ (**2**), (NEt$_4$)$_2$[Ca{O_2C-2,6-(*t*-BuCONH)$_2$$C_6H_3$}$_4$] (**4**), and (NEt$_4$){2,6-(*t*-BuCONH)$_2$$C_6H_3CO_2$} (**3**) are shown in Figure 12. The amide NH signals for **2** appear at 10.2 and 12.5 ppm, and that for **3** appears at 14.7 ppm, which shifted to lower magnetic field than that of the non-hydrogen-bonded NH groups for **2**. The amide NH signal for **4** appears

(49) Carrell, C. J.; Carrell, H. L.; Erlebacher, J.; Glusker, J. P. *J. Am. Chem. Soc.* **1988**, *110*, 8651−8656.
(50) Einspahr, H.; Bugg, C. E. *Acta Crystallogr.* **1981**, *B37*, 1044−1052.
(51) Einspahr, H.; Bugg, C. E. *Metal Ions in Biological System*; Dekker: Basel, Switzerland, 1984; Vol. 17.
(52) Shoji, A.; Kumura, H.; Ozaki, T.; Sugsawa, H.; Deguchi, K. *J. Am. Chem. Soc.* **1996**, *118*, 7604−7607.

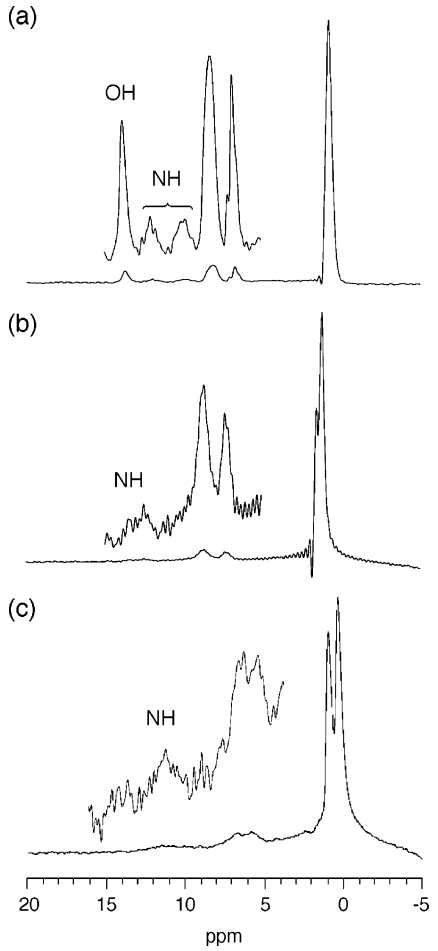

Figure 12. ^{1}H NMR CRAMPS spectra of (a) 2,6-(*t*-BuCONH)$_2$C$_6$H$_3$CO$_2$H (**2**), (b) (NEt$_4$)$_2$[Ca{O$_2$C-2,6-(*t*-BuCONH)$_2$C$_6$H$_3$}$_4$] (**4**), and (c) (NEt$_4$){2,6-(*t*-BuCONH)$_2$C$_6$H$_3$CO$_2$} (**3**) in the solid state.

Table 7. ν(NH) and ν(ND) IR Bands (cm^{-1}) of **2**−**6**

	ν(NH)	ν(ND)
2,6-(*t*-BuCONH)$_2$C$_6$H$_3$CO$_2$H (**2**)	3407	2466
(NEt$_4$){2,6-(*t*-BuCONH)$_2$C$_6$H$_3$CO$_2$} (**3**)	3024	2209
(NEt$_4$)$_2$[Ca{O$_2$C-2,6-(*t*-BuCONH)$_2$C$_6$H$_4$}$_4$] (**4**)	3230	2364
[Tb{O$_2$C-2,6-(*t*-BuNHCO)$_2$C$_6$H$_3$}$_3$·(H$_2$O)$_3$}] (**5**)	3254	2385
(NMe$_4$)[Tb{O$_2$C-2,6-(*t*-BuNHCO)$_2$C$_6$H$_3$}$_4$(thf)] (**6**)	3252	2375

at 12.3 ppm. Thus, the NH···O hydrogen bonds formed in the calcium complex are weaker than that in the carboxylate anion **3**.

Such NH···O hydrogen bonds are also determined by IR spectroscopy in the solid state, as shown in Table 7. Assignments of amide ν(NH) bands are confirmed by using ν(ND) bands with deuterium exchange. The NH band for carboxylic acid **2** appears at 3407 cm^{-1}, indicating the absence of the NH···O hydrogen bond formation. The large low-wavenumber shift of the NH band for carboxylate **3** (3024 cm^{-1}) is due to the strong hydrogen bonding. The slightly shifted NH bands for Ca(II) and Tb(III) complexes correspond to the existence of the weaker NH···O hydrogen bonds, which is revealed by ^{1}H NMR spectroscopy.

Biological Relevance. In the calcium-binding sites of proteins, there is often found mononuclear tetrakis- or tris-(carboxylato) Ca(II) cores with anionic charge.[1] We have attempted to synthesize the tetrakis(carboxylato) complex with bulky benzoate ligands, 2,4,6-Me$_3$C$_6$H$_2$CO$_2$H; however, only the bis(carboxylato) complex is produced. Our doubly amidated benzoate ligand **2** gives mononuclear tetrakis-(carboxylato) complex **4**, which is the first example of a mononuclear Ca(II) complex. Tb(III) ion has an ionic radius similar to that of the Ca(II) ion, and we have isolated mononuclear tris- and tetrakis(carboxylato)−Tb(III) complexes with bulky amide ligands. The amide-containing ligand can prohibit the *anti*-type coordination and induce chelate-type coordination, which induces a mononuclear core. The negatively charged Ca(II) core in the calcium-binding proteins is thought to be stabilized by the NH···O hydrogen bonds to the coordinating carboxylate groups.

We have shown that the NH···O hydrogen-bonded benzoate ligands can bind strongly to Ca(II) or Tb(III) ions in both hydrophobic and hydrophilic conditions. This is because the hydrogen-bonded ligands give a lower pK_a value and the stability constant K_{HL} becomes higher according to eq 3. Calcium-binding proteins have coordinating carboxylate groups to the Ca(II) ion, and they are NH···O hydrogen-bonded with the main chain amide NH groups. These binding proteins have extensively small K_d values; thus, they bind strongly to Ca(II) ions. Our hydrogen-bonded functional analogues clearly indicate that the NH···O hydrogen bonds to coordinating carboxylate groups are quite important for the stabilization of Ca−O bonds in calcium-binding proteins.

Conclusions

Strong intramolecular NH···O hydrogen bonds form between amide groups such as MeCONH and *t*-BuCONH substituted on the *ortho* positions of benzoate and the carboxylate in solution and in the solid state. Such intramolecular hydrogen bonds contribute to the formation of strong Ca(II) and Tb(III) complexes with carboxylates and prevent the dissociation of the calcium−carboxylate and terbium−carboxylate bonds. The crystallographic studies show that our amide-containing ligands prohibit *anti*-type coordination of carboxylate groups and create novel mononuclear Ca(II) and Tb(III) cores which are negatively charged. Our hydrogen-bonded functional analogues clearly indicate that the NH···O hydrogen bonds to coordinating carboxylate groups are one of the important factors for calcium ion management and regulation of coordination geometry in calcium-binding proteins.

Acknowledgment. Support of this work via JSPS Fellowships [for A.O., Grant 2306 (1999-2002)] and a Grant-in-Aid for Scientific Research on Priority Area (A) (Grant 10146231) from the Ministry of Education, Culture, Sports, Science, and Technology, Japan, is gratefully acknowledged.

Supporting Information Available: X-ray crystallographic data in CIF format. This material is available free of charge via the Internet at http://pubs.acs.org.

IC035075T